

This is a repository copy of *The dental calculus metabolome in modern and historic samples*.

White Rose Research Online URL for this paper:

<https://eprints.whiterose.ac.uk/134918/>

Version: Accepted Version

Article:

Velsko, Irina, Overmyer, Katherin, Speller, Camilla Filomena orcid.org/0000-0001-7128-9903 et al. (11 more authors) (2017) The dental calculus metabolome in modern and historic samples. *Metabolomics*. 134. pp. 1-17. ISSN 1573-3890

<https://doi.org/10.1007/s11306-017-1270-3>

Reuse

Items deposited in White Rose Research Online are protected by copyright, with all rights reserved unless indicated otherwise. They may be downloaded and/or printed for private study, or other acts as permitted by national copyright laws. The publisher or other rights holders may allow further reproduction and re-use of the full text version. This is indicated by the licence information on the White Rose Research Online record for the item.

Takedown

If you consider content in White Rose Research Online to be in breach of UK law, please notify us by emailing eprints@whiterose.ac.uk including the URL of the record and the reason for the withdrawal request.

[Click here to view linked References](#)

1
2
3
4
5
6
7
8
9
10
11
12
13
14
15
16
17
18
19
20
21
22
23
24
25
26
27
28
29
30
31
32
33
34
35
36
37
38
39
40
41
42
43
44
45
46
47
48
49
50
51
52
53
54
55
56
57
58
59
60
61
62
63
64
65

1 **Title**
2 The dental calculus metabolome in modern and historic samples

3
4 **Keywords:**
5 Metabolomics; dental plaque; oral microbiome; archaeology; GC-MS; UPLC-MS/MS
6

1
2
3
4 **7 Abstract**
5 8
6 9

7 9 *Introduction:* Dental calculus is a mineralized microbial dental plaque biofilm that forms
8 10 throughout life by precipitation of salivary calcium salts. Successive cycles of dental plaque
9 11 growth and calcification make it an unusually well-preserved, long-term record of host-microbial
10 12 interaction in the archaeological record. Recent studies have confirmed the survival of authentic
11 13 ancient DNA and proteins within historic and prehistoric dental calculus, making it a promising
12 14 substrate for investigating oral microbiome evolution via direct measurement and comparison of
13 15 modern and ancient specimens.

15 16 *Objective:* We present the first comprehensive characterization of the human dental calculus
16 17 metabolome using a multi-platform approach.

18 18 *Methods:* Ultra performance liquid chromatography-tandem mass spectrometry (UPLC-MS/MS)
19 19 quantified 285 metabolites in modern and historic (200 years old) dental calculus, including
20 20 metabolites of drug and dietary origin. A subset of historic samples was additionally analyzed by
21 21 high-resolution gas chromatography-MS (GC-MS) and UPLC-MS/MS for further
22 22 characterization of metabolites and lipids. Metabolite profiles of modern and historic calculus
23 23 were compared to identify patterns of persistence and loss.

25 24 *Results:* Dipeptides, free amino acids, free nucleotides, and carbohydrates substantially decrease
26 25 in abundance and ubiquity in archaeological samples, with some exceptions. Lipids generally
27 26 persist, and saturated and mono-unsaturated medium and long chain fatty acids appear to be
28 27 well-preserved, while metabolic derivatives related to oxidation and chemical degradation are
29 28 found at higher levels in archaeological dental calculus than fresh samples.

31 29 *Conclusions:* The results of this study indicate that certain metabolite classes have higher
32 30 potential for recovery over long time scales and may serve as appropriate targets for oral
33 31 microbiome evolutionary studies.
34 32
35
36
37
38
39
40
41
42
43
44
45
46
47
48
49
50
51
52
53
54
55
56
57
58
59
60
61
62
63
64
65

1
2
3
4 **33 1. Introduction**

5 34 Metabolites are small molecular weight molecules produced by a diverse range of
6 35 enzymatic and chemical reactions, and include products derived from both endogenous and
7 36 exogenous sources. Profiling metabolites in biological systems to define a metabolome is
8 37 increasingly common, as it can provide insight into normal and perturbed metabolic processes
9 38 and their relation to health and disease. Easily obtained human biofluids including serum
10 39 (Psychogios et al. 2011), urine (Bouatra et al. 2013), and saliva (Dame et al. 2015) have been
11 40 extensively profiled to define the range of metabolites that are produced in health, and how their
12 41 levels fluctuate based on changes in activity (Daskalaki et al. 2015), diet (Lankinen et al. 2014),
13 42 drug use (Fleet et al. 2008; Hahn et al. 1972), and disease progression (Yan et al. 2008). These
14 43 studies have made it possible to search for specific metabolites that can act as biomarkers for a
15 44 diverse range of disorders and diseases, including cardiovascular disease (Jensen et al. 2014),
16 45 diabetes (Sysi-Aho et al. 2011), periodontal disease (Barnes et al. 2011; 2009), and cancer
17 46 (Beger 2013).

18 47 Saliva has become an increasingly popular source for metabolite analysis because
19 48 collection is simple, non-invasive, does not require training, and it is abundant and easy to
20 49 resample and store (Dame et al. 2015). Saliva is composed mainly of water, but it also contains a
21 50 wealth of molecules including mucins, proteins, carbohydrates, salts, and metabolites derived
22 51 from serum, local cellular processes, diet, and oral microbes (Zhang et al. 2012). Because of the
23 52 presence of serum-derived molecules, saliva has been used to search for biomarkers both of local
24 53 diseases, such as periodontal disease (Barnes et al. 2011) and oral cancer (Yan et al. 2008), and
25 54 also systemic diseases such as pancreatic and breast cancers (Sugimoto et al. 2010), and
26 55 cardiovascular disease (Foley et al. 2012).

27 56 Metabolites from dental plaque, a microbial biofilm that develops on teeth, may provide
28 57 novel information regarding host-microbiome interactions in health and disease. Dental plaque is
29 58 likely to contain host saliva- and gingival crevicular fluid (GCF)-derived metabolites in addition
30 59 to microbial metabolites, potentially providing a substrate for direct comparison of host and
31 60 microbial activities. For reasons not well understood, dental plaque periodically and rapidly
32 61 mineralizes to form dental calculus, a substance with concrete-like hardness that is immediately
33 62 re-colonized by oral bacteria in a repetitive process (White 1991). Such rapid entombment has
34 63 the potential to trap biomolecules from GCF and saliva as well as oral plaque and dietary and
35 64 environmental debris (Warinner 2016; Warinner et al. 2015).

36 65 Although generally kept to low levels by professional dental hygiene regimens today,
37 66 dental calculus was ubiquitous and relatively abundant in past human populations, as attested by
38 67 dental calculus preserved within archaeological and paleontological collections spanning tens of
39 68 thousands of years, and it is also found on the dentitions of some animal species (Warinner 2016;
40 69 Warinner et al. 2015). Recent biomolecular investigations of ancient dental calculus have
41 70 demonstrated that it contains exceptionally well preserved DNA and proteins from oral biofilm
42 71 species, dietary components, and the host (Warinner, Hendy, et al. 2014; Warinner, Rodrigues, et
43 72 al. 2014), as well as preserved plant microfossils (e.g., pollen, starch granules) and metabolic
44 73 products (e.g. terpenoids) likely originating from dietary and craft activities (Blatt et al. 2011;
45 74 Buckley et al. 2014; Hardy et al. 2012; Radini et al. 2016; Warinner, Rodrigues, et al. 2014).
46 75 Such samples allow deep-time genetic and non-genetic molecular anthropology approaches to
47 76 studying changes in human behavior, evolution of the oral biofilm and disease processes, and co-
48 77 evolution of the oral microbiome and host, which are difficult to study using current *in vitro* and
49 78 *in vivo* technologies alone. Gas-chromatography analyses of dental calculus from Neanderthals

1
2
3
4 79 (Buckley et al. 2014; Radini et al. 2016), pre-agriculturalists (Hardy et al. 2016), and early
5 80 agriculturalists (Hardy et al. 2012) have been used to infer the use of dietary and/or medicinal
6 81 plants; however, to our knowledge, no broad-scale analysis to determine the potential range of
7 82 metabolites trapped in dental calculus has been undertaken.

8 83 Here we present an in-depth, metabolic analysis of a set of historic and modern dental
9 84 calculus samples using a combination of targeted and untargeted approaches to assess the range
10 85 of metabolites that can be extracted from calculus, and how well they persist and preserve over
11 86 time. We validated our results and performed targeted metabolite searches in a subset of historic
12 87 samples for a more thorough assessment of the potential preservation of metabolites of interest.
13 88

16 89 **2. Materials and Methods**

17 90 *2.1 Calculus collection and preparation*

18 91 Fresh dental calculus samples were obtained during routine dental cleaning at the
19 92 University of Oklahoma Periodontology Clinic (n=1) in Oklahoma City, Oklahoma, USA and at
20 93 a private dentistry practice (n=4) in Jaen, Spain (Table 1). Samples were collected by dental
21 94 professionals using a dental scaler following standard calculus removal procedures. All samples
22 95 were obtained under informed consent, and this research was reviewed and approved by the
23 96 University of Oklahoma Health Sciences Center Institutional Review Board (IRB# 4543).
24 97 Historic dental calculus (Figure S1a) was collected from 12 skeletons in the Radcliffe Infirmary
25 98 Burial Ground collection, housed at Oxford Archaeology in Oxford, UK (Table 1). This
26 99 cemetery was used from 1770-c.1855, and the skeletons are not personally identifiable. The oral
27 100 health of each skeleton was recorded with reference to the presence or absence of caries and
28 101 periodontal disease, with reference to (Hillson 1996; Ogden 2005). The sex and approximate age
29 102 at death for each skeleton was estimated following standard osteological criteria (Brooks and
30 103 Suchey 1990; Buckberry and Chamberlain 2002; Ferembach et al. 1980; Lovejoy et al. 1985;
31 104 Phenice 1969; Schwartz 1996) and is presented in Table 1. Genetic sex was further confirmed
32 105 through high-throughput sequencing (HTS) of DNA extracted from additional calculus
33 106 fragments (described below) following previously described methods (Frantz et al. 2016;
34 107 Skoglund et al. 2015; 2013); genetic sex determinations for all twelve samples were consistent
35 108 with those made using osteological approaches. For details see Supplemental Methods.

36 109 After collection, the fresh and historic dental calculus samples were stored frozen and
37 110 transferred on dry ice to Metabolon, Inc. (Durham, NC) for sample processing and metabolite
38 111 extraction and detection by UPLC-MS/MS. A subset of five historic dental calculus samples
39 112 (CS6, CS12, CS18, CS24, and CS46) were additionally analyzed at the Departments of
40 113 Chemistry and Biomolecular Chemistry at the University of Wisconsin (Madison, USA) to
41 114 further characterize metabolites and lipids by high-resolution gas chromatography (GC)-MS and
42 115 UPLC-MS/MS (Table 1).
43 116

44 117 *2.2 Genetic Authentication of a Preserved Oral Microbiome in Historic Samples*

45 118 DNA extracted from a separate fragment of each piece of historic calculus was used to
46 119 assess microbial community composition. DNA was extracted as previously described, but
47 120 omitting phenol-chloroform steps (Warinner, Rodrigues, et al. 2014), and Illumina shotgun
48 121 sequenced (for details see Supplemental Methods). The 16S rRNA gene-identified reads were
49 122 then used to assess microbial community composition at the genus level by closed-reference
50 123 OTU-picking against the GreenGenes v. 13.8 database using UCLUST (Edgar 2010) in QIIME
51 124 v. 1.9 (Caporaso et al. 2010). The Bayesian analysis-based program SourceTracker (Knights et
52 125
53
54
55
56
57
58
59
60
61
62
63
64
65

1
2
3
4 125 al. 2011) was used to estimate the source composition of the microbial community identified by
5 126 QIIME. Human reads were identified by mapping to GRCh38.p10 (GCF_000001405.36) using
6 127 bwa (Meyer et al. 2012) with the flags `aln -l 16500 -o 2 -n 0.01`, duplicate reads were removed,
8 128 and reads mapping to X and Y chromosomes were analyzed for genetic sex determination as
9 129 described above.

10 130 11 131 *2.3 Mass spectrometry and data processing for UPLC-MS/MS*

12 132 Samples (~20 mg) were decalcified in 0.5M EDTA, centrifuged to pellet debris, and
14 133 supernatant prepared using the automated MicroLab STAR® system from Hamilton Company.
15 134 Samples were cleaned and divided into five fractions: two for analysis by two separate reverse
16 135 phase (RP)/UPLC-MS/MS methods with positive ion mode electrospray ionization (ESI), one for
17 136 analysis by RP/UPLC-MS/MS with negative ion mode ESI, one for analysis by HILIC/UPLC-
19 137 MS/MS with negative ion mode ESI, and one sample was reserved for backup. All methods
20 138 utilized a Waters ACQUITY ultra-performance liquid chromatography (UPLC) and a Thermo
21 139 Scientific Q-Exactive high resolution/accurate mass spectrometer interfaced with a heated
22 140 electrospray ionization (HESI-II) source and Orbitrap mass analyzer operated at 35,000 mass
24 141 resolution. For details see Supplemental Methods. Raw data were extracted, peak-identified and
25 142 QC processed using Metabolon's hardware and software. Compounds were identified by
26 143 comparison to library entries of purified standards or recurrent unknown entities. Peaks were
27 144 quantified using area-under-the-curve. Each compound was corrected in run-day blocks by
28 145 registering the medians to equal one (1.00) and normalizing each data point proportionately. For
30 146 specific details about the hardware, software, and libraries used, please see Supplementary
31 147 Materials section 2.6.

32 148 33 149 *2.4 Further characterization of historic calculus by GC-MS and UPLC-MS/MS*

34 150 Five historic dental calculus samples were selected to further investigate metabolites and
36 151 lipids in historic dental calculus samples (Table 1). Following sample pulverization, 15 mg was
37 152 decalcified with 100 uL of 4% Formic acid. Samples were incubated at 4°C with occasional
38 153 shaking for 12 days. Next, 75 uL of 1 M ammonium hydroxide was added, then samples were
39 154 extracted with 350 uL MeOH + 350 uL Acetonitrile (final 2:2:1 Methanol:Acetonitrile:Water).
41 155 Extract was split for metabolite (GC-MS) and lipid (LC-MS) analysis and dried down by vacuum
42 156 centrifugation. For GC-MS analysis molecules were analyzed with electron-impact (EI)-Orbitrap
43 157 full scan of 50-650 m/z range. Lipid LC-MS analysis was performed on a Water's Acquity
44 158 UPLC CSH C18 Column (2.1 mm x 100 mm) with a 5 mm VanGuard Pre-Column Mobile
45 159 coupled to a Q Exactive Focus. Raw files were analyzed using an in-house tool for
47 160 deconvolution of spectra, quantitation, and identification against in-house and NIST 2014
48 161 libraries (GC-MS), or the Thermo Compound Discoverer™ 2.0 application with peak detection,
49 162 retention time alignment, and gap filling (UPLC-MS/MS). Only peaks 10-fold greater than
51 163 solvent blanks were included in the later analysis. The UPLC-MS/MS data was also processed
52 164 through the Global Natural Products Social Molecular Networking pipeline (Wang et al. 2016).
53 165 For details see Supplemental Methods.

54 166 55 167 *2.5 Data analysis*

56 168 Mass normalized data were used for all downstream analyses. Data was normalized as
58 169 follows: values for each sample were normalized by sample mass utilized for extraction, and
59 170 each biochemical was then rescaled to set the median equal to 1. Lastly, missing values were

1
2
3
4 171 imputed with the minimum. First, overall metabolome composition was summarized at the
5 172 super-pathway, sub-pathway, and metabolite levels, and identified metabolites were cross-
6 173 referenced against public databases to obtain KEGG compound identifiers and Human
7 174 Metabolome Database (HMDB) IDs. Next, metabolites found to be ubiquitously present in
8 175 modern samples and ubiquitously absent in historic calculus were compared. Here ubiquity
9 176 among the five modern samples was applied as a measure to identify highly prevalent
10 177 (potentially core) dental calculus metabolites; complete absence of these metabolites among all
11 178 twelve historic samples was used to identify metabolite candidates that may be particularly prone
12 179 to loss or that are unstable and susceptible to degradation through time-dependent taphonomic
13 180 processes. Following this analysis, differential representation of metabolites between historic and
14 181 modern samples was determined using the program Statistical Analysis of Metagenomic Profiles
15 182 (STAMP) (Parks and Beiko 2010; Parks et al. 2014), first including metabolites detected in both
16 183 historic and modern samples, and then again using only those metabolites that were universally
17 184 detected in all seventeen calculus samples. Metabolite profiles of historic and modern samples
18 185 were compared using 2 group analysis of the average quantity of each metabolite and analyzed
19 186 by White's non-parametric two-sided t-test with bootstrapping to determine the difference
20 187 between proportion (DP) with cut-off 95% and Storey's FDR. Differential abundance was
21 188 determined in hierarchical categorization of super-pathway, sub-pathway, and individual
22 189 metabolite. For both analyses corrected p-values (q-values) of ≤ 0.05 together with an effect size
23 190 ≥ 1 were considered significant. Pathway maps were created using iPATH2 (Yamada et al. 2011)
24 191 for metabolites with KEGG compound identifiers. Partial Least Squares Discriminant Analysis
25 192 (PLS-DA) was performed using the R package mixOmics (Rohart et al. 2017) in default settings,
26 193 and Q2 values for the PLS-DAs was calculated in the R package DiscrMiner
27 194 (<https://github.com/gastonstat/DiscrMiner>) using 2 components to match the mixOmics
28 195 calculations, and "leave one out" cross-validation.
29 196

30 197 **3 Results**

31 198 *3.1 Authentication of historic calculus*

32 199 Archaeological specimens are subject to environmental degradation and contamination,
33 200 and thus it is necessary to confirm of the source (e.g., endogenous microbiome vs. exogenous
34 201 environmental microbes) of biomolecules detected in ancient samples. QIIME and
35 202 SourceTracker analyses confirmed excellent biomolecular preservation of an *in situ* oral
36 203 microbial community within the historic dental calculus samples, and 16S rRNA gene sequences
37 204 closely matched those expected for dental plaque communities, with minimal contamination
38 205 from exogenous sources such as soil and skin (Figure S1b). The high proportion of microbes of
39 206 "unknown" source in several historic dental calculus samples is observed in modern calculus
40 207 samples (Ziesemer et al. 2015) (Figure 1b 'Modern'), and is a result of mismatched source
41 208 samples. Several poorly taxonomically characterized oral taxa such as *Methanobrevibacter* and
42 209 *Tissierellaceae* are highly abundant in mature dental calculus biofilms but are infrequently
43 210 detected in healthy oral plaque early biofilms such as the Human Microbiome Project cohort we
44 211 used as source samples. Therefore these genera cannot be confidently assigned to an oral plaque
45 212 source, and are instead attributed to an unknown source.
46 213
47 214

48 215 *3.2 Metabolic pathway coverage in dental calculus*

1
2
3
4 216 A total of 285 metabolites were identified by UPLC-MS/MS in the seventeen dental
5 217 calculus samples, and these were categorized as members of one of eight super-groups: *Amino*
6 218 *acids, Carbohydrates, Cofactors and vitamins, Energy, Lipids, Nucleotides, Peptides,* and
7 219 *Xenobiotics* (Figure 1a; Supplemental Table S1), which were further classified into 69 sub-
8 220 categories. More than half of the metabolites (n=185) were detected in both historic and modern
9 221 calculus samples, demonstrating that metabolites can be recovered from historic dental calculus,
10 222 while 99 metabolites were detected only in modern samples and 1 was detected only in historic
11 223 samples. One hundred ninety-nine metabolites were detected in all 5 modern samples, 97 were
12 224 detected in all 12 historic samples, and 85 were detected in all 17 calculus samples (Table S1). A
13 225 smaller subset of historic calculus was analyzed by GC-MS and LC-MS at the University of
14 226 Wisconsin-Madison; this enabled the identification of 15 additional metabolites and 40
15 227 additional lipids, respectively (Figure 1b; Table S2). For metabolites that were quantified in the
16 228 main analysis and in the smaller subset, we see comparable quantitation despite differences in
17 229 extraction procedures and analysis methods between Metabolon and the University of Wisconsin
18 230 (positive correlation, $R^2 = 0.7$, Supplemental Figure S2). UPLC-MS/MS-identified metabolites
19 231 with KEGG compound identifiers (n=207) were located on a general metabolic pathway map
20 232 (Figure S3) and a map of biosynthesis of secondary metabolites (Figure S4).

21 233 To try to characterize more of the unknown features, we analyzed the LC-MS data
22 234 acquired on the subset of historic calculus through the Global Natural Products Social Molecular
23 235 Networking (GNPS) pipeline (Wang et al. 2016). This online tool searches experimental MS2
24 236 spectra against a large number of publically available spectral libraries and clusters spectra based
25 237 on shared fragment ions. The identified clusters were primarily molecules that had been
26 238 identified previously by Metabolon. Expectedly, we found molecular clusters associated with
27 239 lipid class: for example, phosphatidylcholines clustered within the same molecular network, and
28 240 these molecules shared network connections with sphingomyelins containing phosphocholine
29 241 head groups (Figure S5). We also observed clusters of molecules that could be categorized as
30 242 plasticizers, which had not been identified in the data set by metabolon; however, we suspect
31 243 these molecules were introduced during sample processing. For example, one of these molecules
32 244 - didodecyl 3,3'-thiodipropionate - has been previously reported to be leached from
33 245 polypropylene tubes during organic extractions (Xia et al. 2005).

3.3 Comparison of dental calculus and saliva metabolomes

34 246
35 247 To determine the degree of overlap between metabolites in dental calculus and
36 248 metabolites in saliva, we compared our results to the saliva metabolome. We downloaded a list
37 249 of all metabolites reported in saliva as catalogued in the Human Metabolome Database (Wishart
38 250 et al. 2013) version 3.6 (hmdb.ca) as of February 2017 to use as the known saliva metabolome.
39 251 This list contained 1233 metabolites of endogenous and exogenous origin, spanning the full
40 252 range of super-pathways detected in calculus samples. Just over half, 159, of the 285 metabolites
41 253 detected in calculus (55.7%) were previously included in HMDB's saliva metabolome (Table
42 254 S1), while these 159 metabolites make up just 12.9% of the total metabolites detected in saliva.
43 255 Of the remaining 107 metabolites detected in calculus, 84 have been detected in blood, urine
44 256 and/or cerebrospinal fluid, and 23 have no HMDB identifier. At least one metabolite in each of
45 257 the sub-pathways represented in calculus is not included in the HMDB saliva metabolome.
46 258
47 259

3.4 Metabolite preservation patterns

48 260
49
50
51
52
53
54
55
56
57
58
59
60
61
62
63
64
65

1
2
3
4 261 Among metabolites that are likely endogenous (host or oral microbiome) in origin (i.e.,
5 262 not xenobiotics), metabolite persistence differs by super-pathway in historic samples (Figure 1).
6 263 Overall, historic samples had lower representation in metabolites categorized as *Amino acids*,
7 264 *Vitamins and cofactors*, *Carbohydrates*, *Nucleotides*, and *Peptides* (Figure 2a). In contrast,
8 265 *Lipids* and *Energy* metabolites were generally observed in both historic and modern calculus
9 266 (Figure 2a). Additionally, at a finer scale, certain chemical configurations appear to be lost
10 267 through time, for example N-acetylation, amino acids with positively-charged R-groups, and
11 268 phenyl rings one carbon away from an oxygen. These data suggested a preservation bias that
12 269 could be due to either chemical stability or compound solubility, although it is a possibility that
13 270 low sample amounts limit the detection of certain metabolites.

14 271 To test the hypothesis that preservation is linked to aqueous solubility, we compared the
15 272 differential abundance of metabolites between modern and historic calculus to the predicted
16 273 hydrophobicity of the compounds. The predicted hydrophobicity was extracted from the HMDB,
17 274 which sources the ALOGPS predicted ratio of compound partitioning between 1-octanol and
18 275 water (logP) (Tetko and Bruneau 2004). When plotting fold-change abundance (modern/historic)
19 276 to logP, we observe a significant ($p < 0.001$) negative correlation (Figure 2b), suggesting that
20 277 molecules that are more abundant in modern calculus have lower organic solubility and higher
21 278 aqueous solubility. This result is consistent with our hypothesis that metabolite preservation is in
22 279 part due to aqueous solubility. The exception to our hypothesis, and the outlier in Figure 2b, are
23 280 poly-unsaturated fatty acids (PUFAs), which have high logP but low preservation. Two PUFAs,
24 281 mead acid (20:3n9) and dihomo-linolenate (20:3n3 or n6), were identified in all modern dental
25 282 calculus samples but were not observed in historic samples. The loss of these PUFAs in historic
26 283 calculus may be partially explained by the decreased oxidative stability of fatty acids with
27 284 decreasing saturation (Cosgrove et al. 1987; Rustan and Drevon 2005).

28 285 As yet there are no detailed assessments of metabolite degradation in archaeological
29 286 dental calculus; however, analyses of protein damage patterns in human dental calculus and
30 287 mammoth bone (Cappellini et al. 2012) can be used to draw comparisons with damage patterns
31 288 in calculus metabolites. Warinner, *et al.* (Warinner, Rodrigues, et al. 2014) found that the most
32 289 common protein post-translational modification products in ancient dental calculus are
33 290 deamidation of asparagine, deamidation of glutamine, oxidation of methionine, and conversion
34 291 of N-terminal glutamine to pyroglutamate. Asparagine was detected in all five modern samples
35 292 and eleven historic samples, while the deamidation product aspartate was detected in all
36 293 seventeen samples, and in higher quantity. Glutamine was detected in all modern samples but not
37 294 in historic samples, and its deamination products glutamate and 5-oxoproline were detected in
38 295 higher concentration in all 17 samples, although at much higher concentration in modern than
39 296 historic samples. Oxidation, which is widely documented in the degradation of oil paintings
40 297 (Oakley et al. 2015) and food spoilage (Velasco and Dobarganes 2002) also occurs in dental
41 298 calculus. For example, the ratio of cholesterol and its oxidation product 7-ketocholesterol was
42 299 reversed between modern and historic calculus, and kynurenin, an oxidation product of
43 300 tryptophan that is known to accumulate in archaeological bone over time (Cappellini et al. 2012),
44 301 was detected in historic calculus while tryptophan was absent. In contrast, methionine was
45 302 detected in all seventeen samples, and was much more abundant in modern samples, while the
46 303 oxidation product methionine sulfoxide was detected in all five modern samples and in only two
47 304 historic samples, in all cases at lower concentrations. Free methionine sulfoxide may be unstable
48 305 and subject to further rapid breakdown.
49 306

3.5 Lipid 2-hydroxylation as an indicator of calculus age

Four 2-hydroxylated lipids were detected in all calculus samples—2-hydroxyadipate, 2-hydroxystearate, 2-hydroxypalmitate, and 2-hydroxyglutarate—and the first three are more abundant in ancient than modern samples. The only metabolite detected in historic but not modern samples was 2-hydroxydecanoate (detected in 10 of the 12 historic samples), while the parent molecule decanoate was not detected in any of our samples. In contrast, 3-hydroxylated and 2,3-hydroxylated lipids are more abundant in modern than historic samples. The increased presence of 2-hydroxylated lipids in ancient samples suggests that this modification may increase over time. The difference in patterns of lipid hydroxylation between ancient and modern calculus suggests that in some cases 3-hydroxylation may switch to 2-hydroxylation.

3.6 Differentially abundant metabolites in ancient and modern calculus

To further define the differences in metabolic functions preserved through time, we compared the metabolites present in both modern and ancient calculus samples at the super-pathway, sub-pathway, and individual metabolite levels using STAMP. Principal components analysis demonstrated distinct separation of modern and historic samples (Figure 3a) with tight clustering of historic samples along PC1 and PC2, while modern samples were more distributed, suggesting that loss of metabolites through time results in a more uniform metabolite profile between samples than may have originally existed. Comparing the mean proportions of individual metabolites detected in at least one modern and one historic sample, 161 were significantly more abundant ($q \leq 0.05$) in one sample set, yet only 21 additionally had an effect size of ≥ 1.0 (Figure 3b, Table S3 bold metabolites). When considering only the metabolites that were universally present in all five modern and all twelve historic samples (Table S3, superscript 'c'), a slightly different set of metabolites and metabolic pathways are differentially abundant. Historic and modern samples still separate distinctly in PCA (Figure S6a), but many more metabolites have a significant difference in mean proportions (Figure S6b).

We then examined differences in proportion of super-pathways, sub-pathways, and individual metabolites present in at least one modern and historic sample to better understand the patterns of preservation and loss through time. The proportion of *Lipids* was significantly higher in ancient than modern calculus samples, suggesting that non-polar, chemically inert molecules are particularly stable through time (Figure 4a). On the other hand, the proportion of *Amino acids*, *Carbohydrates*, *Cofactors and vitamins*, and *Xenobiotics* were significantly higher in modern calculus (Figure 4a), demonstrating substantial loss and/or degradation of metabolites in these super-pathways over time. The super-pathway *Peptides* was excluded from analysis using this method because its near total absence in historic samples resulted in very few possible comparisons.

As expected from the super-pathway differential abundances, many of the sub-pathways with greater proportional representation in historic calculus were related to lipid metabolism (Figure 4b). The sterols include cholesterol and its oxidation products 4-cholesten-3-one, 7-hydroxycholesterol (alpha or beta), and 7-ketocholesterol, which is consistent with the expectation that increased oxidation will occur over time. *Guanidino and acetamido metabolism* comprised a greater proportion of historic sample metabolites due to overrepresentation of 4-guanidinobutanoate, a product of arginine and putrescine metabolism. Several of the sub-pathways with greater proportional representation in modern samples can be explained by a single metabolite, which manifests at the metabolite level (Figure 4b), and these include *Nicotinate and nicotinamide metabolism*, *Pyrimidine metabolism*, and *Food component/plant*. A

1
2
3
4 353 single metabolite each comprises the *Chemical* and *Drug* sub-pathways, sulfate and salicylate,
5 354 respectively. With respect to the latter, salicylate is abundant in modern pharmaceuticals, but
6 355 may have been consumed medicinally in the form of willow bark tea by the historical population,
7 356 especially given the fact that they were buried in a hospital-associated cemetery. Salicylates are
8 357 also naturally found in a variety of fruits, vegetables, herbs, and spices; however at levels far
9 358 below the therapeutic doses typical of modern pharmaceuticals (Castillo-García et al. 2015).
10 359 Alternatively, the salicylates in the historic calculus samples may be a plant root-derived product
11 360 (Badri and Vivanco 2009), resulting from the diffusion highly soluble, small organic acids into
12 361 the calculus from burial soil.

13 362 In contrast to the large number of sub-pathways representing a significantly higher
14 363 proportion of metabolites between historic and modern calculus, only 6 individual metabolites
15 364 were significantly differentially represented between historic and modern calculus (Figure 4c).
16 365 Modern calculus had significantly higher proportions of nicotinate, orotate, stachydrine, alanine,
17 366 and glucose (Figure 4c). Both nicotinate and orotate may be taken as a dietary supplement, while
18 367 stachydrine (proline betaine), is a plant metabolite that is not metabolized by mammals (Lever et
19 368 al. 1994), but is common in citrus fruits and orange juice (Atkinson et al. 2007). Low abundance
20 369 of stachydrine in historic calculus may relate to dietary differences between these modern and
21 370 historic populations, or to differential preservation. Alanine, the smallest amino acid, and glucose
22 371 may be lost through high solubility. The lipid 2-hydroxystearate was the only metabolite of
23 372 significantly greater proportion in historic samples, even though several 2-hydroxylated lipids
24 373 had greater relative abundance in historic samples.

25 374 In addition to endogenous metabolites, several xenobiotics found to be present only in
26 375 modern calculus samples are from food and pharmacologic agents introduced to or popularized
27 376 in European populations in the 20th century, including the artificial sweeteners acesulfame,
28 377 saccharin, and arabitol/xylitol. Additionally, theobromine, an alkylid present in coffee, tea, and
29 378 chocolate, was also only detected in modern calculus, suggesting that consumption of these
30 379 products by the historic population was absent or low, despite their increasing availability in
31 380 Europe in the 1800s, or that this metabolite poorly preserves over time.

32 381 *3.7 Potential for maintenance of biological signatures in calculus metabolite profiles*

33 382 Unlike saliva, dental calculus does not represent a snapshot of a specific time and specific
34 383 metabolic state, but rather it represents a life history in which specific profiles may be diluted out
35 384 by fluctuating metabolic processes throughout an individual's life, loss of unstable metabolites
36 385 over time, and random chance with respect to the entrapment of xenobiotics and dietary
37 386 compounds. However, distinct metabolic signatures related to biological variables such as sex
38 387 (Takeda et al. 2009), oral health status (Barnes et al. 2009; 2011), and oral biofilm microbial
39 388 composition (Takahashi et al. 2010) have been reported in saliva, GCF, and oral plaque samples,
40 389 all of which are likely to contribute to the metabolite profile in dental calculus. Therefore, we
41 390 assessed differences in metabolic profiles between calculus from different age groups, sex, and
42 391 oral health status by partial least squares discriminant analysis (PLS-DA) (Q2 values Table S4),
43 392 and, further, looked for metabolites that could be specifically attributed to bacterial activity.

44 393 No differences were found in the metabolite profile between age groups, between males
45 394 and females, between samples from caries-affected and caries-free dentitions, or between
46 395 samples from periodontal disease-affected and non-affected individuals when considering
47 396 metabolites detected in at least one historic and one modern calculus sample (Figure 5a), or
48 397 metabolites universally present in all 17 samples (Figure S8a). However, there was a distinct
49 398

1
2
3
4 399 separation of modern and historic samples in each comparison so we repeated PLS-DA using
5 400 only historic sample data. PLS-DA separated historic samples based on sex, age, caries status
6 401 and periodontal disease status when using metabolites detected in at least one historic sample
7 402 (Figure 5b) and when using only metabolites present in all 12 historic samples (Figure S8b).
8 403 Applying PSL-DA to universally detected metabolites in only the *Lipid* and *Energy* classes, (the
9 404 best-preserved classes in historic samples, Figure 1a) separated samples based on time period
10 405 rather than biological category (Figure S8c). These results suggest that biological categories in
11 406 modern and historic calculus samples cannot be directly compared, yet patterns of biological
12 407 differences are maintained through time.

13 408 Similarly, no metabolites could be specifically attributed to bacterial processes, but
14 409 several metabolites, including isovalerate, valerate, lactate, cadaverine and putrescine, are
15 410 known metabolic products of oral bacteria (Scully et al. 1997; Takahashi 2015). Dipicolinate,
16 411 which was detected in all modern and all historic samples, is the major component of bacterial
17 412 spore capsules, and may indicate that bacterial endospore development occurs in mature plaque
18 413 biofilms, or during plaque mineralization. Sulfate is abundant in GCF due to break-down of
19 414 sulfur-containing amino acids by the oral biofilm, and is produced during anaerobic
20 415 methanogenesis in oral plaque, however, we observed no correlation between the relative
21 416 abundance of the oral methanogen *Methanobrevibacter* and sulfate levels (Figure S9) in our
22 417 samples, and the very high abundance of sulfate in historic relative to modern calculus suggests
23 418 an exogenous source. Oxford topsoil sulfur concentrations where the cemetery was located are in
24 419 the 70th percentile across England and Wales (Rawlins et al. 2012), and sulfates in the soil and
25 420 ground water of the cemetery may leach into the calculus by the same processes through which
26 421 highly water-soluble metabolites are leached out of calculus.
27
28
29
30
31
32

33 423 **4 Discussion**

34 424 Our results derived from the non-targeted assessment of metabolites present in dental
35 425 calculus from both modern and historic samples demonstrate the significant potential of calculus
36 426 as a material for metabolomics and lipidomic studies. The wide range of metabolic categories
37 427 covered (amino acids, carbohydrates, cofactors and vitamins, energy, lipids, nucleic acids,
38 428 peptides, xenobiotics), and the variety of sources of metabolites (host, microbial, diet) are on par
39 429 with those reported in saliva (Barnes et al. 2011) and GCF (Barnes et al. 2009) using similar
40 430 metabolite detection platforms. Similar to the study defining the saliva metabolome (Dame et al.
41 431 2015), we found using multiple metabolomics platforms (5 different methods by Metabolon, Inc.
42 432 and 2 by UW-Madison) increased the diversity of compounds we detected. However, unlike
43 433 Dame *et al* (2015), we found more metabolites by LC than GC methodologies, which was likely
44 434 due to the low-abundance of molecules with higher aqueous solubility in the historic calculus
45 435 that were analyzed by GC-MS. Although we found lower representation of aqueous-soluble
46 436 molecules, in general calculus preserves a wide variety of molecules from the oral cavity and
47 437 could be useful proxy for oral biofluids in archaeological samples. Calculus also provides an
48 438 opportunity to co-investigate host and microbial activity, which is increasingly recognized as
49 439 important to understanding cellular physiology and disease pathology (Takahashi 2015).

50 440 Saliva has been shown to preserve an individualized metabolic signature throughout daily
51 441 routine (Wallner-Liebmann et al. 2016) and dental calculus, which contains salivary components,
52 442 has the potential to preserve aspects of individual profiles over longer periods of time. While
53 443 only five modern calculus samples were included in this study, PCA analysis revealed substantial
54 444 metabolite profile diversity within these samples (Figure 2a). It therefore appears that modern
55
56
57
58
59
60
61
62
63
64
65

1
2
3
4 445 calculus may preserve individual phenotypes, although to investigate this, studies with larger
5 446 sample sizes are needed to further assess this potential. Historic samples, in contrast, cluster
6 447 much more tightly in the PCA, suggesting that individual phenotypes may be lost through
7 448 metabolite degradation and loss over time. However, we were able to distinguish metabolic
8 449 profile differences in historic samples between sex, age, and oral health status of the individuals
9 450 by PLS-DA, demonstrating maintenance of individual profiles despite metabolite loss. It may
10 451 then be possible to investigate differences in specific metabolite profile in historic samples,
11 452 which could contribute to our understanding of disease demographics and evolution.

12
13
14 453 Relatively little is known about the process of age-related protein degradation in
15 454 archaeological samples, yet other historic samples provide some insight. Asparagine readily
16 455 deamidates via cyclization to succinimidyl within chain; however, this mechanism is unavailable
17 456 to the free amino acid. Under experimental heating, asparagine undergoes rapid hydrolysis (Crisp
18 457 et al. 2013), and it is therefore probable that the free asparagine seen in the historic samples is
19 458 derived from hydrolysis of peptides. Free glutamine and glutamic acid can undergo cyclisation to
20 459 pyroglutamic acid even at low temperatures (Nagana Gowda et al. 2015). However, although
21 460 pyroglutamate (pGlu; 5-oxoproline) is present at higher levels in the historic samples, it is too
22 461 low to account for all the loss of all glutamic acid. This consistent pattern suggests that there is a
23 462 contributing pool of degrading proteins, generating free amino acids which are undergoing
24 463 modification, either in chain (e.g., asparagine deamidation) or once hydrolysed to terminal
25 464 positions or as free amino acids (e.g., pyroglutamate). The majority of these low molecular
26 465 weight, high solubility products are then likely lost from the calculus matrix. It is possible that
27 466 some are so entrapped within the crystal matrix that they may persist as free amino acids and
28 467 pyroglutamate, and this could be assessed by monitoring the level of racemization (Crisp et al.
29 468 2013).

30
31
32
33 469 Persistence of the Energy metabolites is unexpected given that most of the molecules in
34 470 this category are small and water soluble, and therefore expected to be lost through time. Alpha-
35 471 ketoglutarate may be produced by degradation of glutamate, which appears to be occurring in
36 472 calculus as discussed in our results, and it may form stabilizing complexes with calcium, which
37 473 is highly abundant in the predominantly calcium-phosphate mineral matrix of dental calculus.
38 474 However, we speculate that these Energy metabolites may be fungal- or plant-derived
39 475 compounds from the burial soil. Both plant roots and their associated mycorrhizal fungi secrete
40 476 organic acids including citrate, malate, and oxalate (Badri and Vivanco 2009; Klugh and
41 477 Cumming 2007), which are more abundant than expected in our historic samples. We expect that
42 478 the endogenous Energy metabolites are lost over time through solubility, yet organic acids
43 479 present in the soil from roots and fungi may diffuse into the historic calculus samples, and thus it
44 480 appears that these metabolites are not lost through time. This concern may be addressed in future
45 481 experiments by looking at preservation of small organic acids in historic calculus samples from
46 482 individuals who were never buried in soil, such as from crypt burials, and from archaeological
47 483 samples that have been in storage for varying periods of time.

48
49
50
51
52 484 Lipids, particularly unmodified, saturated classes, are some of the best-preserved
53 485 metabolites in historic calculus, and appear to be particularly stable over time. Therefore, lipid
54 486 analyses may be a promising focus for historic calculus studies. Although not a common focus in
55 487 salivary or oral biofilm metabolomics studies, lipids are a versatile class of molecule with a
56 488 broad range of physiological properties and actions. They play roles in local (intracellular)
57 489 (Nishizuka 1995) and long-distance (hormone) cell signaling (Xavier et al. 2016), have both pro-
58 490 and anti-inflammatory properties (Bennett and Gilroy 2016), and are the major components of
59
60
61
62
63
64
65

1
2
3
4 491 cell membranes, where their composition influences cell membrane function (Zalba and Hagen
5 492 2017). Bacterial membrane lipid content varies by species (López-Lara and Geiger 2016), and
6 493 may indicate bacterial physiological status (Darveau et al. 2004), while pathogenesis of the
7 494 periodontal disease-associated oral bacteria *Porphyromonas gingivalis* is influenced by host cell
8 495 membrane lipid composition (Min Wang and Hajishengallis 2008). The role of lipid mediators in
9 496 the initiation and resolution of periodontal disease inflammation is currently under investigation
10 497 (Bartold and Van Dyke 2013), and the wealth of lipids detected in calculus may be valuable to
11 498 studies of both host and microbial pathophysiology.

12 499 Although we were unable to specifically identify bacterial contributions to the calculus
13 500 metabolome, there are some metabolites suggestive of mature oral biofilm activity. Dipicolinate,
14 501 which is the major capsule component of bacterial endospores, is a highly stable molecule, as
15 502 evidenced by the long-term viability of endospores (Yung et al. 2007). To our knowledge, the
16 503 inferred presence of endospores in calculus is a novel finding, as we were unable to find any
17 504 references to the presence of bacterial endospores in oral plaque or dental calculus. Members of
18 505 several Gram-positive genera that reside in the mouth have close relatives known to form spores,
19 506 including *Actinomyces* (Gao and Gupta 2012), and *Filifactor* (Vos et al. 2011), and since many
20 507 oral bacteria have not yet been genetically or physiologically characterized, it is possible that
21 508 several oral species do have the ability to form spores. Calcification of the biofilm may induce a
22 509 stress response in these species that initiates endospore formation, which would explain the
23 510 abundance of dipicolinate in dental calculus.

24 511 Additionally, studies aiming to characterize salivary biomarkers of periodontal disease
25 512 have identified several pathways with an apparent bacterial source that contain promising
26 513 metabolite candidates for disease biomarkers (Kuboniwa et al. 2016; Sakanaka et al. 2017), and
27 514 we have identified several of these in our calculus. Phenylalanine, succinate, hydrocinnamate,
28 515 cadaverine, and putrescine are markers of periodontal disease that were reduced in saliva when
29 516 supragingival plaque was removed, suggesting they were largely produced by bacteria (Sakanaka
30 517 et al. 2017), and we detected each of these molecules. This demonstrates that bacterial metabolic
31 518 products are present in calculus, and may offer insight into mature biofilm activity. This could be
32 519 useful in studying how bacterial metabolism influences oral disease, as periodontal disease-
33 520 associated oral plaque has community structure and activity much more similar to that of fully
34 521 mature biofilms such as are found in calculus, than to healthy site subgingival plaque or
35 522 supragingival plaque (Wade 2013), yet the presence of calculus alone is not a reflection of
36 523 periodontal disease status (i.e., three of the five modern calculus samples were collected from
37 524 teeth with no evidence of periodontal disease).

38 525 In sum, our results demonstrate that dental calculus contains an abundance of endogenous
39 526 and exogenous metabolites, and that a wide range of these metabolites preserve well through
40 527 time. Dental calculus therefore has significant potential to provide novel insights into human
41 528 diet, physiology, and microbiome activity in both modern and historic samples, permitting
42 529 human evolutionary and human-microbiome co-evolutionary studies with a deep-time
43 530 perspective. Larger sample sizes and samples from additional temporal and cultural contexts as
44 531 well as from varying burial and storage conditions are needed to further address metabolite
45 532 preservation and presence/absence patterns. The excellent preservation of dental calculus in
46 533 archaeological collections, however, means that there is ample opportunity to expand metabolite-
47 534 based studies of dental calculus into the recent and distant past.

535 536 **Acknowledgments**

1
2
3
4
5
6
7
8
9
10
11
12
13
14
15
16
17
18
19
20
21
22
23
24
25
26
27
28
29
30
31
32
33
34
35
36
37
38
39
40
41
42
43
44
45
46
47
48
49
50
51
52
53
54
55
56
57
58
59
60
61
62
63
64
65

537 The authors thank Mark Gibson, Tom Gilbert, Chris Gosden, Stuart Gould, Lauren McIntyre,
538 Anita Radini, William Wade, and Helen Webb for assistance with sample and data collection.
539 We would like to acknowledge The Danish National High-Throughput DNA Sequencing Centre
540 for sequencing the samples. This work was supported by the Oxford University Fell Fund
541 143/108 (to G.L. and C.W.), the European Research Council ERC-2013-StG 337574-UNDEAD
542 (to G.L.), the National Institutes of Health R01GM089886 (to C.M.L., C.W., and K.S.), the
543 National Science Foundation BCS-1516633 and BCS-1643318 (to C.W.), and R35GM118110
544 (to J.J.C.) and the National Library of Medicine T15LM007359 (to K.A.O.).

546 **Compliance with ethical standards**

547
548 **Conflict of interest** All authors declare that they have no conflict of interest.

549
550 **Ethical approval** The study was approved by the Institutional Review Board for Human
551 Research Participant Protection at the University of Oklahoma [IRB#4543] and was performed
552 in accordance with the 1964 Helsinki declaration and its later amendments.

553
554 **Informed consent** Informed consent was obtained from all modern participants in the study
555 prior to the collection of dental calculus.

556
557 **Data availability**

558 All data generated or analyzed during this study are included in this published article (and its
559 supplementary information files).

561 **Tables**

562

Table 1. Summary of sample demographic and health information and analyses performed

ID	Age ^a	Sex ^b	Smoker	Oral Health	Sampled Tooth	Analyses performed
<i>Modern</i>						
OK1010	40	M	Former	+ PD	- caries, + PD	UPLC-MS/MS
ES28	31	F	Current	+ caries, + GV	- caries, - PD	UPLC-MS/MS
ES29	30	M	No	+ caries, + GV	- caries, - PD	UPLC-MS/MS
ES20	23	M	Current	+ caries, + GV	- caries, - PD	UPLC-MS/MS
ES15	71	M	Former	+ caries, + PD	- caries, + PD	UPLC-MS/MS
<i>Historic</i>						
CS06	36-45	M	N/A	+ caries, + PD	- caries, - PD	UPLC-MS/ MS ^d ; GC-MS
CS12	36-45	M	N/A	+ caries, + PD	- caries, - PD	UPLC-MS/MS ^d ; GC-MS
CS18	36-45	M	N/A	- caries, + PD	- caries, - PD	UPLC-MS/MS ^d ; GC-MS
CS24	36-45	F	N/A	+ caries, + PD	+ caries, + PD	UPLC-MS/MS ^d ; GC-MS
CS46	>45	F	N/A	+ caries, + PD	- caries, - PD	UPLC-MS/MS ^d ; GC-MS
CS20	36-45	M	N/A	+ caries, + PD	- caries, - PD	UPLC-MS/MS
CS21	26-35	M	N/A	- caries, - PD	- caries, - PD	UPLC-MS/MS
CS23	26-35	F	N/A	+ caries, + PD	- caries, - PD	UPLC-MS/MS
CS30	18-25	F	N/A	+ caries, - PD	- caries, - PD	UPLC-MS/MS
CS31	36-45	F	N/A	+ caries, + PD	- caries, - PD	UPLC-MS/MS
CS39	36-45	M	N/A	- caries, + PD	- caries, - PD	UPLC-MS/MS
CS40	>45	F	N/A	- caries, - PD	- caries, - PD	UPLC-MS/MS

^aAge of skeletons used for historical calculus sampling is based on osteological indicators and is a range estimate. ^bHistorical skeleton sex estimate is based on both osteological indicators and DNA sequencing, and was in concurrence between the two methods. ^dUPLC-MS/MS was performed twice; the first at Metabolon, Inc. and the second at the University of Wisconsin-Madison. PD, periodontal disease; GV, gingivitis; N/A, not available; +, present; -, absent.

563

564
565
566

Figure legends

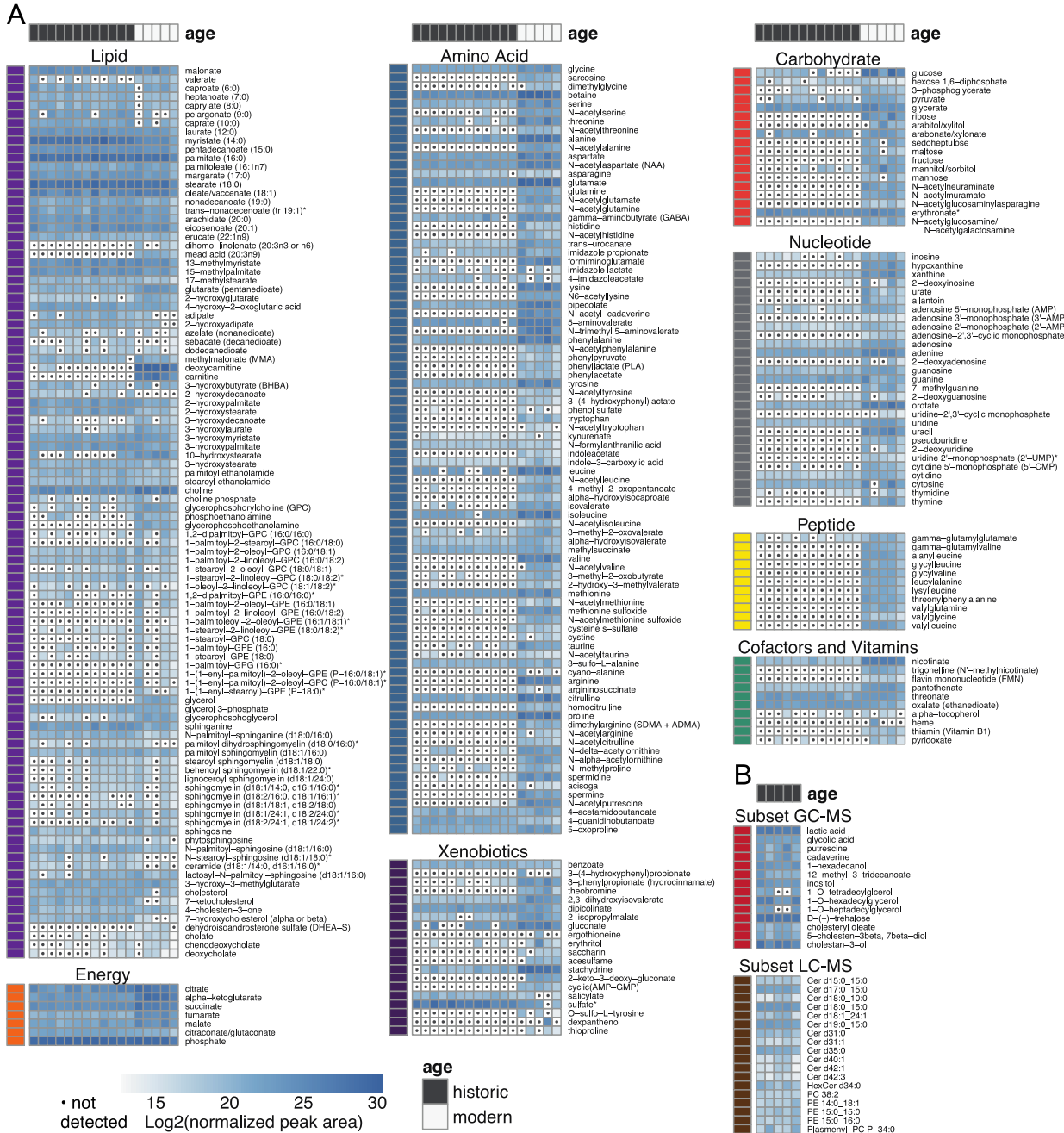


Fig. 1 Heat map summary of metabolites observed in modern and historic dental. Metabolites were quantified by area under the curve and normalized to mass of sample extracted. **a** UPLC-MS/MS-detected metabolites. Samples were hierarchically clustered, and log2 transformed values are presented above, grouped by super-pathway. **b** Metabolites detected by GC-MS and LC-MS in historic calculus. Non-filled cells containing a dot indicate the compound was not detected.

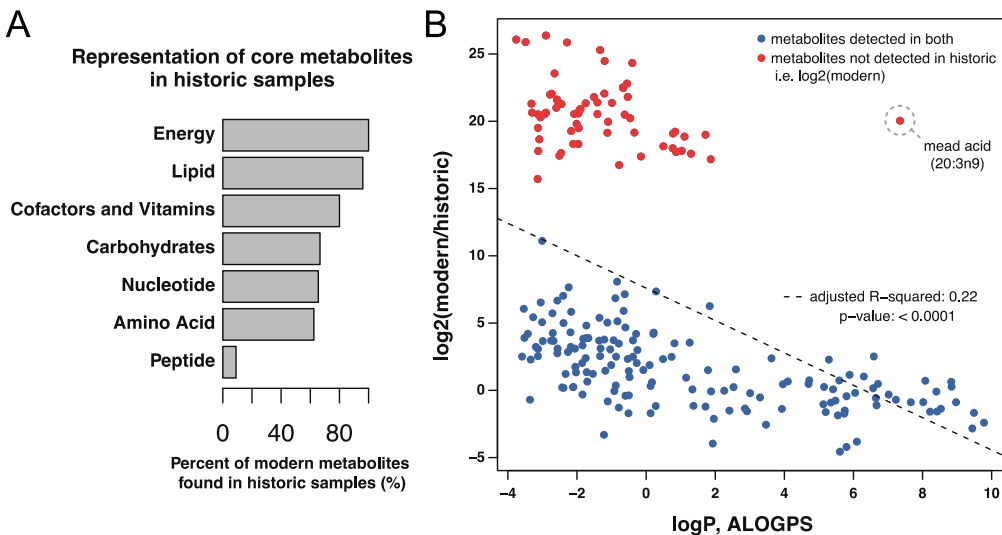


Fig. 2 Compound preservation is correlated with aqueous solubility. **a** Percent of high ubiquity metabolites in modern calculus that were also recovered in at least one historic calculus sample. *Peptides* exhibit the poorest representation in historic dental calculus, with only 9% of the peptides observed to be present in all five modern calculus samples also detected in any historic sample. By contrast, *Lipids* and *Energy* (TCA cycle) super-pathways exhibit high representation in historic calculus, with >96% of compounds found in all five modern samples also recovered from historic dental calculus. *Xenobiotics*, which largely comprise dietary and pharmaceutical compounds, are not shown. **b** The \log_2 fold-change (modern/historic) of metabolite abundance vs. the 1-octanol vs. water partition coefficient ($\log P$), estimated with the ALOGPS tool. In the cases where metabolites were only detected in modern calculus, the \log_2 values (not fold-change) were plotted relative to $\log P$. The fitted linear model showed a significant effect ($p < 0.0001$) of $\log P$ on metabolite fold-change with an adjusted R^2 of 0.22. The outlier from this trend was mead acid (20:3n9).

590

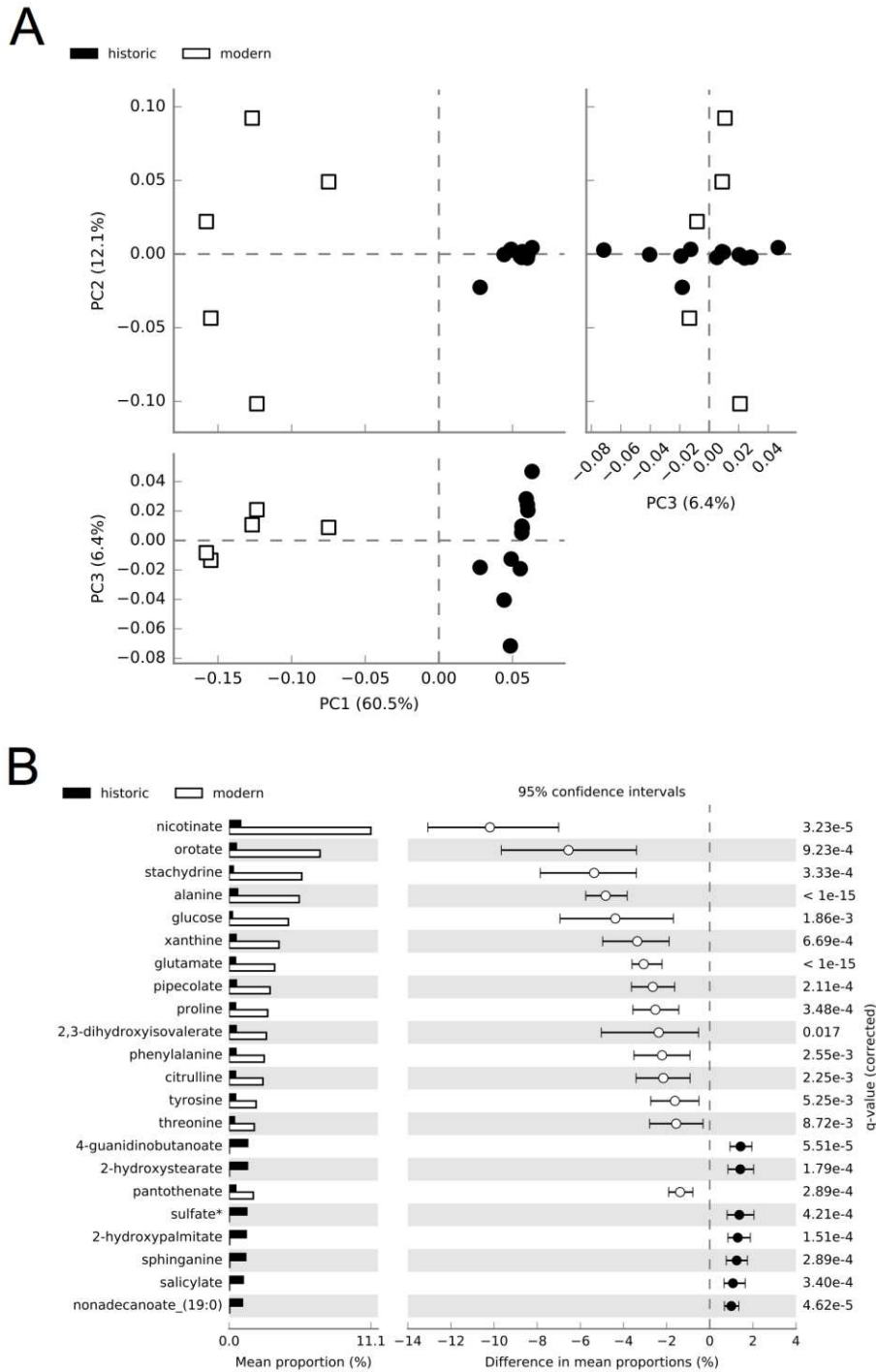


Fig. 3 Differences exist in mean proportions of metabolites detected in at least one historic and one modern dental calculus sample. **a** Principal components analysis distinctly separates modern and historic calculus samples. **b** Metabolites with significant differences ($q \leq 0.05$, effect size of ≥ 1.0) in mean proportions between historic and modern calculus.

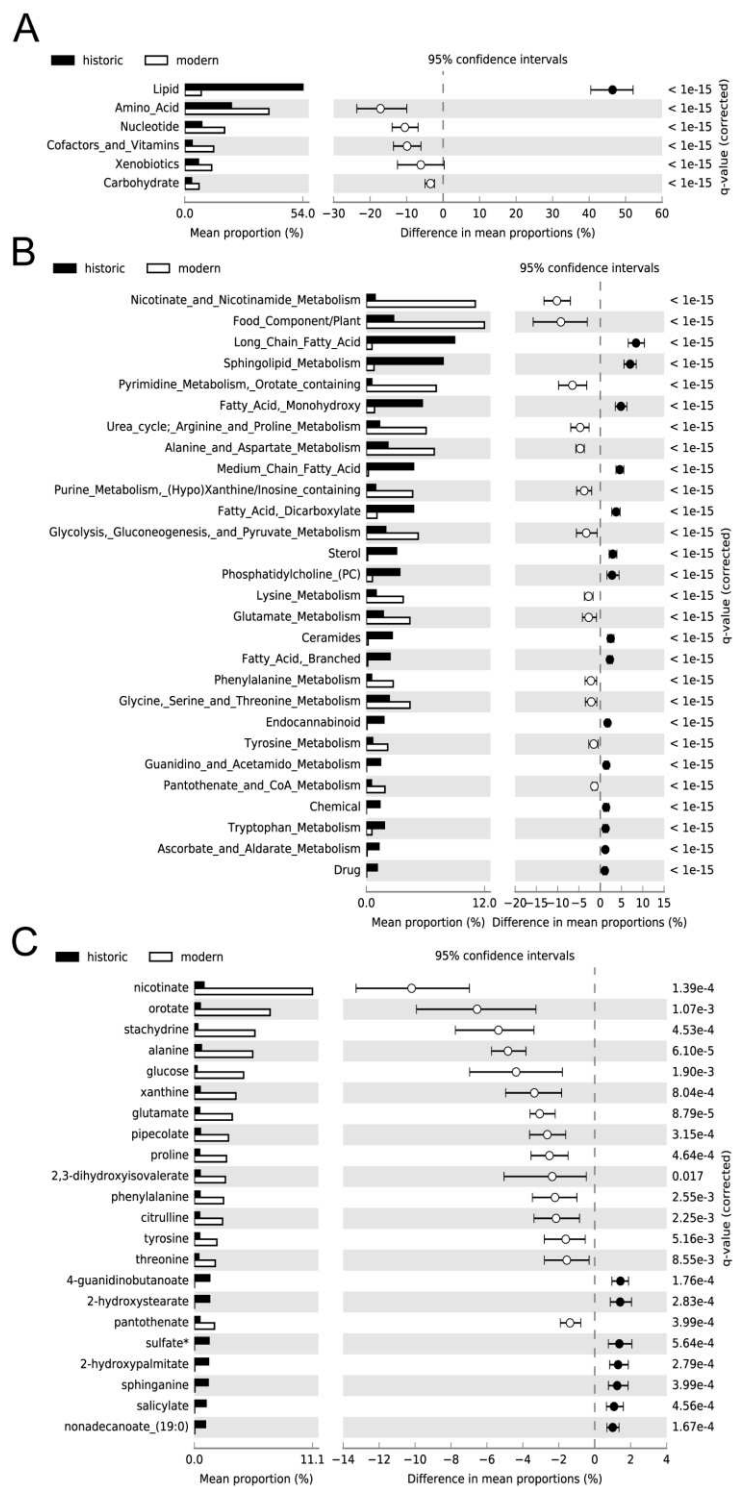


Fig. 4 Differences exist in proportions of super-pathways, sub-pathways, and metabolites represented in at least one historic and one modern dental calculus sample. Significantly different ($q \leq 0.05$, effect size of ≥ 1.0) proportions of **a** Super-pathways, **b** Sub-pathways, and **c** metabolites. Individual metabolites between historic and modern samples.

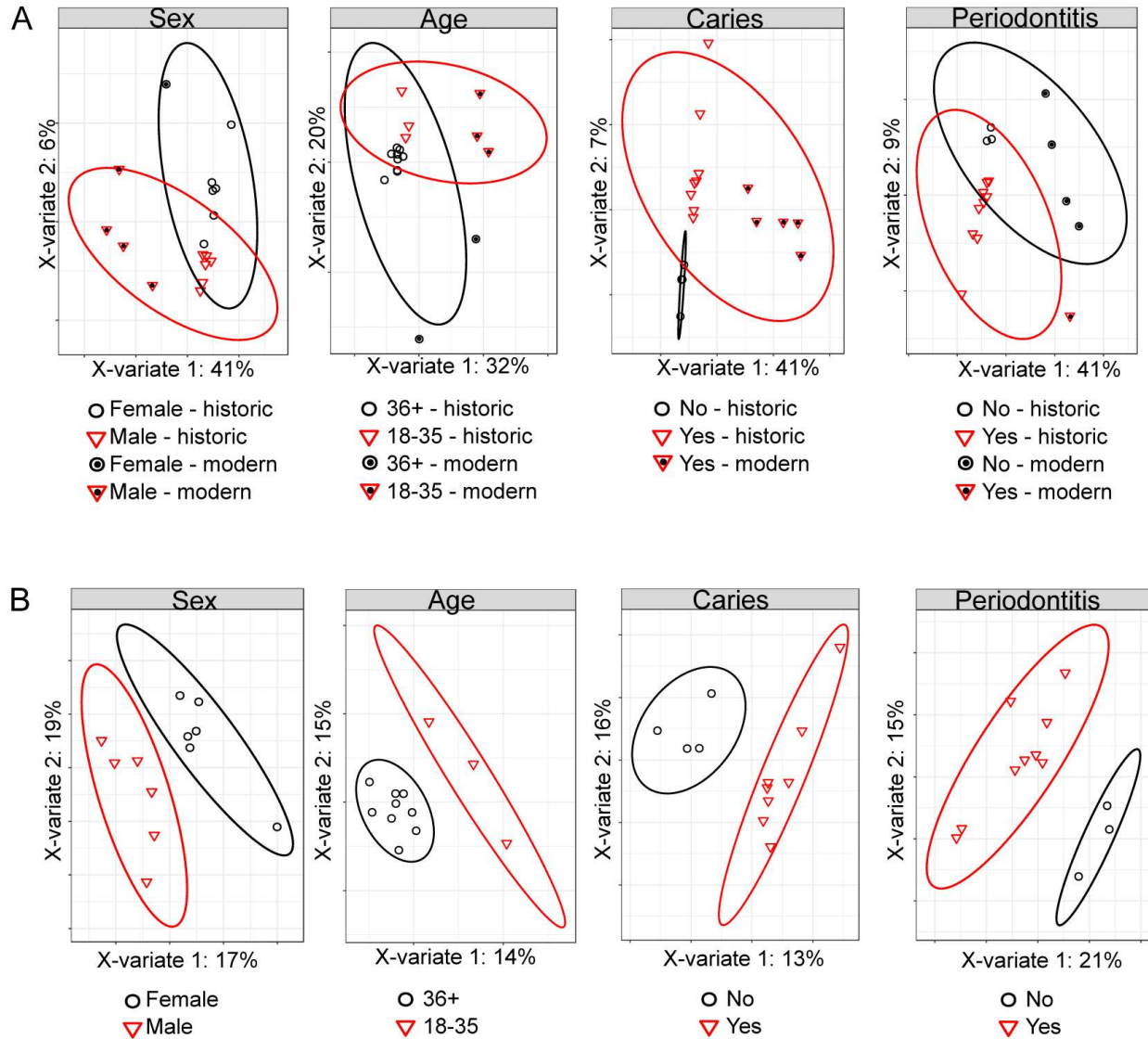


Fig. 5 Partial least squares discriminant analysis of metabolites detected at least one modern and one historic calculus sample. **a** Calculus samples cluster based on time period rather than biological category (sex, age, caries status and periodontal disease status) when including all metabolites detected in at least one modern and one historic sample. **b** Historic calculus samples cluster based on biological category (sex, age, caries status and periodontal disease status) when including all metabolites detected in at least one historic sample. Ellipses indicate 95% confidence intervals.

1
2
3
4 **616 Supplementary Tables**

5 617
6 618 **Table S1.** Raw UPLC-MS/MS data from Metabolon. Tab 1 (OrigScale) contains data
7 619 normalized in terms of raw area counts. Tab 2 (MassNormImp) contains data normalized as
8 620 follows: values for each sample are normalized by sample mass available/used for extraction,
9 621 then each biochemical is rescaled to set the median equal to 1, and missing values are imputed
10 622 with the minimum. (Excel sheet).
11 623

12 624 **Table S2.** Raw Data from the University of Wisconsin-Madison. Tab 1 Metabolites detected by
13 625 GC-MS. Tab 2 Metabolites detected by UPLC-MS/MS. (Excel sheet).
14 626

15 627 **Table S3.** Differential abundance of UPLC-MS/MS-identified metabolites between modern and
16 628 historic dental calculus. (Word doc).
17 629

18 630 Table S4. Q2 values for all PLS-DAs.
19 631

20 632 **Supplementary Figures**

21 633
22 634 **Fig. S1** Historic calculus samples contain oral bacterial community profiles. **a** Historic calculus
23 635 on teeth from CS18 prior to sampling. **b** Percent of bacterial community in calculus samples
24 636 attributable to distinct environmental sources by SourceTracker analysis. Modern samples from
25 637 Ziesemer et al. (2015), demonstrate that a high proportion of the microbial community assigned
26 638 to an “Unknown” source is characteristic of dental calculus. CS6 failed to build DNA libraries
27 639 with the AccuPrimePFX polymerase.
28 640

29 641 **Fig. S2** Comparison of quantified metabolites from samples analyzed by Metabolon, Inc. and
30 642 Wisconsin-Madison. Five calculus samples were analyzed by GC-MS and LC-MS in Madison,
31 643 Wisconsin; the relative quantitation obtained on these methods was significantly correlated with
32 644 results from Metabolon, Inc. (linear regression, $p < 0.001$).
33 645

34 646 **Fig. S3.** Representation of diverse metabolic pathways preserved in calculus. Large circles
35 647 represent metabolites identified in calculus. Black rings around large circles indicate the
36 648 metabolite was detected in historic calculus.
37 649

38 650 **Fig. S4.** Representation of pathways for biosynthesis of secondary metabolites preserved in
39 651 calculus. Large circles represent metabolites identified in calculus. Black rings around large
40 652 circles indicate the metabolite was detected in historic calculus.
41 653

42 654 **Fig. S5** Global Natural Products Social Molecular Networking (GNPS) analysis of UPLC-
43 655 MS/MS spectra (Wisconsin subset) clusters compounds containing phosphocholine head groups.
44 656 This network of molecular clusters (nodes) contains molecules with putative identifications (dark
45 657 blue) to phosphatidylcholines and sphingomyelins containing phosphocholine. The edges denote
46 658 at least 3 matching fragments between spectra and a cosine score of >0.8 .
47 659

48 660 **Fig. S6.** Differences exist in mean proportions of metabolites universally detected in all historic
49 661 and modern dental calculus samples. **a** Principal components analysis distinctly separates
50
51
52
53
54
55
56
57
58
59
60
61
62
63
64
65

1
2
3
4 662 modern and historic calculus samples. **b** Metabolites with significant differences ($q \leq 0.05$, effect
5 663 size of ≥ 1.0) in mean proportions between historic and modern calculus.
6
7 664

8 665 **Fig. S7.** Differences exist in proportions of super-pathways, sub-pathways, and metabolites
9 666 universally detected in all historic and modern dental calculus samples. Significantly different (q
10 667 ≤ 0.05 , effect size of ≥ 1.0) proportions of **a** Super-pathways, **b** Sub-pathways, and **c** Individual
11 668 metabolites between historic and modern samples.
12
13 669

14 670 **Fig. S8.** Partial least squares discriminant analysis of metabolites universally present in calculus
15 671 samples. **a** Calculus samples cluster based on time period rather than biological category (sex,
16 672 age, caries status and periodontal disease status) when including metabolites detected in all
17 673 seventeen calculus samples. **b** Historic calculus samples cluster based on biological category
18 674 (sex, age, caries status and periodontal disease status) when including metabolites detected in all
19 675 twelve historic samples. **c** When using only universally detected metabolites in the *Lipid* and
20 676 *Energy* categories (pathways with the best representation in historic samples), it was still not
21 677 possible to discriminate samples based on biological category, although the separation between
22 678 historic and modern samples was reduced slightly compared to **a**. Ellipses indicate 95%
23 679 confidence intervals.
24
25 680

26 681 **Fig. S9.** Comparison of sulfate abundance and the relative abundance of the oral sulfate-
27 682 producing genus, *Methanobrevibacter*, shown using **a** linear and **b** log scales.
28 683 *Methanobrevibacter* relative abundance was estimated using 16S rRNA gene sequence counts,
29 684 and no correlation was observed with sulfate abundance. *Methanobrevibacter* was not detected
30 685 in CS18.
31
32
33
34
35
36
37
38
39
40
41
42
43
44
45
46
47
48
49
50
51
52
53
54
55
56
57
58
59
60
61
62
63
64
65

1
2
3
4 **References**

- 5 687
6 688 Atkinson, W., Downer, P., Lever, M., Chambers, S. T., & George, P. M. (2007). Effects of
7 689 orange juice and proline betaine on glycine betaine and homocysteine in healthy male
8 690 subjects. *European Journal of Nutrition*, 46(8), 446–452. doi:10.1007/s00394-007-0684-5
9 691 Badri, D. V., & Vivanco, J. M. (2009). Regulation and function of root exudates. *Plant, Cell &*
10 692 *Environment*, 32(6), 666–681. doi:10.1111/j.1365-3040.2009.01926.x
11 693 Barnes, V. M., Ciancio, S. G., Shibly, O., Xu, T., Devizio, W., Trivedi, H. M., et al. (2011).
12 694 Metabolomics Reveals Elevated Macromolecular Degradation in Periodontal Disease.
13 695 *Journal of Dental Research*, 90(11), 1293–1297. doi:10.1177/0022034511416240
14 696 Barnes, V. M., Teles, R., Trivedi, H. M., Devizio, W., Xu, T., Mitchell, M. W., et al. (2009).
15 697 Acceleration of purine degradation by periodontal diseases. *Journal of Dental Research*,
16 698 88(9), 851–855. doi:10.1177/0022034509341967
17 699 Bartold, P. M., & Van Dyke, T. E. (2013). Periodontitis: a host-mediated disruption of microbial
18 700 homeostasis. Unlearning learned concepts. *Periodontology 2000*, 62, 203–217.
19 701 Beger, R. D. (2013). A review of applications of metabolomics in cancer. *Metabolites*, 3(3),
20 702 552–574. doi:10.3390/metabo3030552
21 703 Bennett, M., & Gilroy, D. W. (2016). Lipid Mediators in Inflammation. *Microbiology Spectrum*,
22 704 4(6). doi:10.1128/microbiolspec.MCHD-0035-2016
23 705 Blatt, S. H., Redmond, B. G., Cassman, V., & Sciulli, P. W. (2011). Dirty teeth and ancient
24 706 trade: Evidence of cotton fibres in human dental calculus from Late Woodland, Ohio.
25 707 *International Journal of Osteoarchaeology*, 21(6), 669–678. doi:10.1002/oa.1173
26 708 Bouatra, S., Aziat, F., Mandal, R., Guo, A. C., Wilson, M. R., Knox, C., et al. (2013). The human
27 709 urine metabolome. *PLoS ONE*, 8(9), e73076. doi:10.1371/journal.pone.0073076
28 710 Brooks, S., & Suchey, J. M. (1990). Skeletal age determination based on the os pubis: A
29 711 comparison of the Acsádi-Nemeskéri and Suchey-Brooks methods. *Human Evolution*, 5(3),
30 712 227–238. doi:10.1007/BF02437238
31 713 Buckberry, J. L., & Chamberlain, A. T. (2002). Age estimation from the auricular surface of the
32 714 ilium: A revised method. *American Journal of Physical Anthropology*, 119(3), 231–239.
33 715 doi:10.1002/ajpa.10130
34 716 Buckley, S., Usai, D., Jakob, T., Radini, A., & Hardy, K. (2014). Dental Calculus Reveals
35 717 Unique Insights into Food Items, Cooking and Plant Processing in Prehistoric Central Sudan.
36 718 *PLoS ONE*, 9(7), e100808–10. doi:10.1371/journal.pone.0100808
37 719 Caporaso, J. G., Kuczynski, J., Stombaugh, J., Bittinger, K., Bushman, F. D., Costello, E. K., et
38 720 al. (2010). QIIME allows analysis of high-throughput community sequencing data. *Nature*
39 721 *Methods*, 7(5), 335–336. doi:10.1038/nmeth.f.303
40 722 Cappellini, E., Jensen, L. J., Szklarczyk, D., Ginolhac, A., da Fonseca, R. A. R., Stafford, T. W.,
41 723 et al. (2012). Proteomic analysis of a pleistocene mammoth femur reveals more than one
42 724 hundred ancient bone proteins. *Journal of Proteome Research*, 11(2), 917–926.
43 725 doi:10.1021/pr200721u
44 726 Castillo-García, M. L., Aguilar-Caballos, M. P., & Gómez-Hens, A. (2015). Determination of
45 727 acetylsalicylic acid and its major metabolites in bovine urine using ultra performance liquid
46 728 chromatography. *Journal of Chromatography B*, 985, 85–90.
47 729 doi:10.1016/j.jchromb.2015.01.026
48 730 Cosgrove, J. P., Church, D. F., & Pryor, W. A. (1987). The kinetics of the autoxidation of
49 731 polyunsaturated fatty acids. *Lipids*, 22(5), 299–304.
50
51
52
53
54
55
56
57
58
59
60
61
62
63
64
65

- 1
2
3
4 732 Crisp, M., Demarchi, B., Collins, M., Morgan-Williams, M., Pilgrim, E., & Penkman, K. (2013).
5 733 Isolation of the intra-crystalline proteins and kinetic studies in *Struthio camelus* (ostrich)
6 734 eggshell for amino acid geochronology. *Quaternary Geochronology*, *16*, 110–128.
7 735 doi:10.1016/j.quageo.2012.09.002
8
9 736 Dame, Z. T., Aziat, F., Mandal, R., Krishnamurthy, R., Bouatra, S., Borzouie, S., et al. (2015).
10 737 The human saliva metabolome. *Metabolomics*, *11*(6), 1864–1883. doi:10.1007/s11306-015-
11 738 0840-5
12
13 739 Darveau, R. P., Pham, T. T. T., Lemley, K., Reife, R. A., Bainbridge, B. W., Coats, S. R., et al.
14 740 (2004). *Porphyromonas gingivalis* Lipopolysaccharide Contains Multiple Lipid A Species
15 741 That Functionally Interact with Both Toll-Like Receptors 2 and 4. *Infection and Immunity*,
16 742 *72*(9), 5041–5051. doi:10.1128/IAI.72.9.5041-5051.2004
17
18 743 Daskalaki, E., Blackburn, G., Kalna, G., Zhang, T., Anthony, N., & Watson, D. (2015). A Study
19 744 of the Effects of Exercise on the Urinary Metabolome Using Normalisation to Individual
20 745 Metabolic Output. *Metabolites*, *5*(1), 119–139. doi:10.3390/metabo5010119
21 746 Edgar, R. C. (2010). Search and clustering orders of magnitude faster than BLAST.
22 747 *Bioinformatics*, *26*(19), 2460–2461. doi:10.1093/bioinformatics/btq461
23
24 748 Ferembach, D., Schwindezky, I., & Stoukal, M. (1980). Recommendation for Age and Sex
25 749 Diagnoses of Skeletons. *Journal of Human Evolution*, *9*, 517–549.
26 750 Fleet, J. C., Gliniak, C., Zhang, Z., Xue, Y., Smith, K. B., McCreedy, R., & Adedokun, S. A.
27 751 (2008). Serum metabolite profiles and target tissue gene expression define the effect of
28 752 cholecalciferol intake on calcium metabolism in rats and mice. *The Journal of Nutrition*,
29 753 *138*(6), 1114–1120.
30
31 754 Foley, J. D., III, Sneed, J. D., Steinhubl, S. R., Kolasa, J., Ebersole, J. L., Lin, Y., et al. (2012).
32 755 Oral fluids that detect cardiovascular disease biomarkers. *Oral Surgery, Oral Medicine, Oral*
33 756 *Pathology and Oral Radiology*, *114*(2), 207–214. doi:10.1016/j.oooo.2012.03.003
34
35 757 Frantz, L. A. F., Mullin, V. E., Pionnier-Capitan, M., Lebrasseur, O., Ollivier, M., Perri, A., et al.
36 758 (2016). Genomic and archaeological evidence suggest a dual origin of domestic dogs.
37 759 *Science*, *352*(6290), 1228–1231. doi:10.1126/science.aaf3161
38
39 760 Gao, B., & Gupta, R. S. (2012). Phylogenetic framework and molecular signatures for the main
40 761 clades of the phylum Actinobacteria. *Microbiology and Molecular Biology Reviews*, *76*(1),
41 762 66–112. doi:10.1128/MMBR.05011-11
42 763 Hahn, T. J., Hendin, B. A., Scharp, C. R., & Haddad, J. G. (1972). Effect of chronic
43 764 anticonvulsant therapy on serum 25-hydroxycalciferol levels in adults. *The New England*
44 765 *Journal of Medicine*, *287*(18), 900–904. doi:10.1056/NEJM197211022871803
45
46 766 Hardy, K., Buckley, S., Collins, M. J., Estalrich, A., Brothwell, D., Copeland, L., et al. (2012).
47 767 Neanderthal medics? Evidence for food, cooking, and medicinal plants entrapped in dental
48 768 calculus. *Die Naturwissenschaften*, *99*(8), 617–626. doi:10.1007/s00114-012-0942-0
49
50 769 Hardy, K., Radini, A., Buckley, S., Sarig, R., Copeland, L., Gopher, A., & Barkai, R. (2016).
51 770 Dental calculus reveals potential respiratory irritants and ingestion of essential plant-based
52 771 nutrients at Lower Palaeolithic Qesem Cave Israel. *Quaternary International*, *398*(c), 129–
53 772 135. doi:10.1016/j.quaint.2015.04.033
54 773 Hillson, S. (1996). *Dental Anthropology*. Cambridge: Cambridge University Press.
55 774 doi:10.1017/CBO9781139170697
56
57 775 Jensen, M. K., Bertoia, M. L., Cahill, L. E., Agarwal, I., Rimm, E. B., & Mukamal, K. J. (2014).
58 776 Novel metabolic biomarkers of cardiovascular disease. *Nature Reviews Endocrinology*,
59 777 *10*(11), 659–672. doi:10.1038/nrendo.2014.155
60
61
62
63
64
65

- 1
2
3
4 778 Klugh, K. R., & Cumming, J. R. (2007). Variations in organic acid exudation and aluminum
5 779 resistance among arbuscular mycorrhizal species colonizing *Liriodendron tulipifera*. *Tree*
6 780 *Physiology*, 27(8), 1103–1112. doi:10.1093/treephys/27.8.1103
7
8 781 Knights, D., Kuczynski, J., Charlson, E. S., Zaneveld, J., Mozer, M. C., Collman, R. G., et al.
9 782 (2011). Bayesian community-wide culture-independent microbial source tracking. *Nature*
10 783 *Methods*, 8(9), 761–763. doi:10.1038/nmeth.1650
11 784 Kuboniwa, M., Sakanaka, A., Hashino, E., Bamba, T., Fukusaki, E., & Amano, A. (2016).
12 785 Prediction of Periodontal Inflammation via Metabolic Profiling of Saliva. *Journal of Dental*
13 786 *Research*, 95(12), 1381–1386. doi:10.1177/0022034516661142
14 787 Lankinen, M., Kolehmainen, M., Jääskeläinen, T., Paananen, J., Joukamo, L., Kangas, A. J., et
15 788 al. (2014). Effects of whole grain, fish and bilberries on serum metabolic profile and lipid
16 789 transfer protein activities: a randomized trial (Sysdimet). *PLoS ONE*, 9(2), e90352.
17 790 doi:10.1371/journal.pone.0090352
18 791 Lever, M., Sizeland, P.C.B., Bason, L. M., Hayman, C. M., & Chambers, S. T. (1994). Glycine
19 792 betine and proline betaine in human blood and urine. *Biochimica et biophysica acta*, 1200,
20 793 259–264.
21 794 Lovejoy, C. O., Meindl, R. S., Pryzbeck, T. R., & Mensforth, R. P. (1985). Chronological
22 795 metamorphosis of the auricular surface of the ilium: A new method for the determination of
23 796 adult skeletal age at death. *American Journal of Physical Anthropology*, 68(1), 15–28.
24 797 doi:10.1002/ajpa.1330680103
25 798 López-Lara, I. M., & Geiger, O. (2016). Bacterial lipid diversity. *Biochimica et biophysica acta*.
26 799 doi:10.1016/j.bbali.2016.10.007
27 800 Meyer, M., Kircher, M., Gansauge, M.-T., Li, H., Racimo, F., Mallick, S., et al. (2012). A high-
28 801 coverage genome sequence from an archaic Denisovan individual. *Science*, 338(6104), 222–
29 802 226. doi:10.1126/science.1224344
30 803 Nagana Gowda, G. A., Gowda, Y. N., & Raftery, D. (2015). Massive glutamine cyclization to
31 804 pyroglutamic acid in human serum discovered using NMR spectroscopy. *Analytical*
32 805 *chemistry*, 87(7), 3800–3805. doi:10.1021/ac504435b
33 806 Nishizuka, Y. (1995). Protein kinase C and lipid signaling for sustained cellular responses. *The*
34 807 *FASEB Journal*, 9(7), 484–496. doi:10.1096/fj.1530-6860
35 808 Oakley, L. H., Casadio, F., Shull, K. R., & Broadbelt, L. J. (2015). Microkinetic modeling of the
36 809 autoxidative curing of an alkyd and oil-based paint model system. *Applied Physics A*, 121(3),
37 810 869–878. doi:10.1007/s00339-015-9363-1
38 811 Ogden, A. (2005). A New and Simple System for the Recording of Periodontal Disease in
39 812 Skeletal Material (pp. 1–1). Presented at the British Association for Biological Anthropology
40 813 and Osteoarchaeology.
41 814 Parks, D. H., & Beiko, R. G. (2010). Identifying biologically relevant differences between
42 815 metagenomic communities. *Bioinformatics*, 26(6), 715–721.
43 816 doi:10.1093/bioinformatics/btq041
44 817 Parks, D. H., Tyson, G. W., Hugenholtz, P., & Beiko, R. G. (2014). STAMP: statistical analysis
45 818 of taxonomic and functional profiles. *Bioinformatics*, 30(21), 3123–3124.
46 819 doi:10.1093/bioinformatics/btu494
47 820 Phenice, T. W. (1969). A newly developed visual method of sexing the os pubis. *American*
48 821 *Journal of Physical Anthropology*, 30(2), 297–301. doi:10.1002/ajpa.1330300214
49 822 Psychogios, N., Hau, D. D., Peng, J., Guo, A. C., Mandal, R., Bouatra, S., et al. (2011). The
50 823 human serum metabolome. *PLoS ONE*, 6(2), e16957. doi:10.1371/journal.pone.0016957
51
52
53
54
55
56
57
58
59
60
61
62
63
64
65

- 1
2
3
4 824 Radini, A., Buckley, S., Rosas, A., Estalrich, A., la Rasilla, de, M., & Hardy, K. (2016).
5 825 Neanderthals, trees and dental calculus: new evidence from El Sidró n. *Antiquity*, *90*(350),
6 826 290–301. doi:10.15184/aqy.2016.21
7
8 827 Rawlins, B. G., McGrath, S. P., Scheib, A., Breward, N., Cave, M. R., Lister, B., et al. (2012).
9 828 *The advanced soil geochemical atlas of England and Wales*. British Geological Survey.
10 829 Rohart, F., Gautier, B., Singh, A., & Le Cao, K.-A. (2017). mixOmics (draft1): an R package for
11 830 'omics feature selection and multiple data integration. *bioRxiv*, 108597. doi:10.1101/108597
12 831 Rustan, A. C., & Drevon, C. A. (2005). *Fatty Acids: Structures and Properties*. *Encyclopedia of*
13 832 *Life Sciences*. John Wiley & Sons, Ltd. doi:10.1038/npg.els.0003894
14 833 Sakanaka, A., Kuboniwa, M., Hashino, E., Bamba, T., Fukusaki, E., & Amano, A. (2017).
15 834 Distinct signatures of dental plaque metabolic byproducts dictated by periodontal
16 835 inflammatory status. *Scientific Reports*, *7*, 42818. doi:10.1038/srep42818
17 836 Schwartz, J. H. (1996). *Skeleton keys: An introduction to human skeletal morphology,*
18 837 *development, and analysis*. Oxford University Press. doi:10.1007/BF02735270
19 838 Scully, C., el-Maaytah, M., Porter, S. R., & Greenman, J. (1997). Breath odor: etiopathogenesis,
20 839 assessment and management. *European Journal of Oral Sciences*, *105*(4), 287–293.
21 840 Skoglund, P., Ersmark, E., Palkopoulou, E., & Dalén, L. (2015). Ancient wolf genome reveals an
22 841 early divergence of domestic dog ancestors and admixture into high-latitude breeds. *Current*
23 842 *biology : CB*, *25*(11), 1515–1519. doi:10.1016/j.cub.2015.04.019
24 843 Skoglund, P., Storå, J., Götherström, A., & Jakobsson, M. (2013). Accurate sex identification of
25 844 ancient human remains using DNA shotgun sequencing. *Journal of Archaeological Science*,
26 845 *40*(12), 4477–4482. doi:10.1016/j.jas.2013.07.004
27 846 Sugimoto, M., Wong, D. T., Hirayama, A., Soga, T., & Tomita, M. (2010). Capillary
28 847 electrophoresis mass spectrometry-based saliva metabolomics identified oral, breast and
29 848 pancreatic cancer-specific profiles. *Metabolomics*, *6*(1), 78–95. doi:10.1007/s11306-009-
30 849 0178-y
31 850 Sysi-Aho, M., Ermolov, A., Gopalacharyulu, P. V., Tripathi, A., Seppänen-Laakso, T.,
32 851 Maukonen, J., et al. (2011). Metabolic regulation in progression to autoimmune diabetes.
33 852 *PLoS Computational Biology*, *7*(10), e1002257. doi:10.1371/journal.pcbi.1002257
34 853 Takahashi, N. (2015). Oral Microbiome Metabolism: From "Who Are They?" to "What Are
35 854 They Doing?." *Journal of Dental Research*.
36 855 Takahashi, N., Washio, J., & Mayanagi, G. (2010). Metabolomics of Supragingival Plaque and
37 856 Oral Bacteria. *Journal of Dental Research*, *89*(12), 1383–1388.
38 857 doi:10.1177/0022034510377792
39 858 Takeda, I., Stretch, C., Barnaby, P., Bhatnager, K., Rankin, K., Fu, H., et al. (2009).
40 859 Understanding the human salivary metabolome. *NMR in Biomedicine*, *22*(6), 577–584.
41 860 doi:10.1002/nbm.1369
42 861 Tetko, I. V., & Bruneau, P. (2004). Application of ALOGPS to predict 1-octanol/water
43 862 distribution coefficients, logP, and logD, of AstraZeneca in-house database. *Journal of*
44 863 *Pharmaceutical Sciences*, *93*(12), 3103–3110. doi:10.1002/jps.20217
45 864 Velasco, J., & Dobarganes, C. (2002). Oxidative stability of virgin olive oil - Velasco - 2002 -
46 865 European Journal of Lipid Science and Technology - Wiley Online Library. *European*
47 866 *Journal of Lipid Science and Technology*, *104*(9-10), 661–676. doi:10.1002/1438-
48 867 9312(200210)104:9/10<661::AID-EJLT661>3.0.CO;2-D
49 868 Vos, P., Garrity, G., Jones, D., Krieg, N. R., Ludwig, W., Rainey, F. A., et al. (2011). *Bergey's*
50 869 *Manual of Systematic Bacteriology*.
51
52
53
54
55
56
57
58
59
60
61
62
63
64
65

- 1
2
3
4 870 Wade, W. G. (2013). The oral microbiome in health and disease. *Pharmacological Research*,
5 871 69(1), 137–143. doi:10.1016/j.phrs.2012.11.006
6
7 872 Wallner-Liebmann, S., Tenori, L., Mazzoleni, A., Dieber-Rotheneder, M., Konrad, M.,
8 873 Hofmann, P., et al. (2016). Individual Human Metabolic Phenotype Analyzed by. *Journal of*
9 874 *Proteome Research*, 15, 1787–1793.
10 875 doi:10.1021/acs.jproteome.5b01060/suppl_file/pr5b01060_si_001.pdf
11 876 Wang, Min, & Hajishengallis, G. (2008). Lipid raft-dependent uptake, signalling and
12 877 intracellular fate of *Porphyromonas gingivalis* in mouse macrophages. *Cellular*
13 878 *Microbiology*, 10(10), 2029–2042. doi:10.1111/j.1462-5822.2008.01185.x
14 879 Wang, Mingxun, Carver, J. J., Phelan, V. V., Sanchez, L. M., Garg, N., Peng, Y., et al. (2016).
15 880 Sharing and community curation of mass spectrometry data with Global Natural Products
16 881 Social Molecular Networking. *Nature biotechnology*, 34(8), 828–837. doi:10.1038/nbt.3597
17 882 Warinner, C. (2016). Dental Calculus and the Evolution of the Human Oral Microbiome. *Journal*
18 883 *of the California Dental Association*, 44(7), 411–420.
19 884 Warinner, C., Hendy, J., Speller, C., Cappellini, E., Fischer, R., Trachsel, C., et al. (2014). Direct
20 885 evidence of milk consumption from ancient human dental calculus. *Scientific Reports*, 4,
21 886 7104. doi:10.1038/srep07104
22 887 Warinner, C., Rodrigues, J. F. M., Vyas, R., Trachsel, C., Shved, N., Grossmann, J., et al. (2014).
23 888 Pathogens and host immunity in the ancient human oral cavity. *Nature Genetics*, 46(4), 336–
24 889 344. doi:10.1038/ng.2906
25 890 Warinner, C., Speller, C., & Collins, M. J. (2015). A new era in palaeomicrobiology: prospects
26 891 for ancient dental calculus as a long-term record of the human oral microbiome. *Phil. Trans.*
27 892 *R. Soc. B*, 370, 20130376.
28 893 White, D. J. (1991). Processes contributing to the formation of dental calculus. *Biofouling*, 4(1-
29 894 3), 209–218. doi:10.1080/08927019109378211
30 895 Wishart, D. S., Jewison, T., Guo, A. C., Wilson, M., Knox, C., Liu, Y., et al. (2013). HMDB
31 896 3.0—The Human Metabolome Database in 2013. *Nucleic Acids Research*, 41(D1), D801–
32 897 D807. doi:10.1093/nar/gks1065
33 898 Xavier, A. M., Anunciato, A. K. O., Rosenstock, T. R., & Glezer, I. (2016). Gene Expression
34 899 Control by Glucocorticoid Receptors during Innate Immune Responses. *Frontiers in*
35 900 *Endocrinology*, 7, 31. doi:10.3389/fendo.2016.00031
36 901 Xia, Y.-Q., Patel, S., Bakhtiar, R., Franklin, R. B., & Doss, G. A. (2005). Identification of a new
37 902 source of interference leached from polypropylene tubes in mass-selective analysis. *Journal*
38 903 *of the American Society for Mass Spectrometry*, 16(3), 417–421.
39 904 doi:10.1016/j.jasms.2004.11.020
40 905 Yamada, T., Letunic, I., Okuda, S., Kanehisa, M., & Bork, P. (2011). iPath2.0: interactive
41 906 pathway explorer. *Nucleic Acids Research*, 39(suppl), W412–W415. doi:10.1093/nar/gkr313
42 907 Yan, S.-K., Wei, B.-J., Lin, Z.-Y., Yang, Y., Zhou, Z.-T., & Zhang, W.-D. (2008). A
43 908 metabonomic approach to the diagnosis of oral squamous cell carcinoma, oral lichen planus
44 909 and oral leukoplakia. *Oral Oncology*, 44(5), 477–483.
45 910 doi:10.1016/j.oraloncology.2007.06.007
46 911 Yung, P. T., Shafaat, H. S., Connon, S. A., & Ponce, A. (2007). Quantification of viable
47 912 endospores from a Greenland ice core. *FEMS Microbiology Ecology*, 59(2), 300–306.
48 913 doi:10.1111/j.1574-6941.2006.00218.x
49 914 Zalba, S., & Hagen, Ten, T. L. M. (2017). Cell membrane modulation as adjuvant in cancer
50 915 therapy. *Cancer treatment reviews*, 52, 48–57. doi:10.1016/j.ctrv.2016.10.008
51
52
53
54
55
56
57
58
59
60
61
62
63
64
65

1
2
3
4
5
6
7
8
9
10
11
12
13
14
15
16
17
18
19
20
21
22
23
24
25
26
27
28
29
30
31
32
33
34
35
36
37
38
39
40
41
42
43
44
45
46
47
48
49
50
51
52
53
54
55
56
57
58
59
60
61
62
63
64
65

Zhang, A., Sun, H., & Wang, X. (2012). Saliva Metabolomics Opens Door to Biomarker Discovery, Disease Diagnosis, and Treatment. *Applied Biochemistry and Biotechnology*, 168(6), 1718–1727. doi:10.1007/s12010-012-9891-5

Ziesemer, K. A., Mann, A. E., Sankaranarayanan, K., Schroeder, H., Ozga, A. T., Brandt, B. W., et al. (2015). Intrinsic challenges in ancient microbiome reconstruction using 16S rRNA gene amplification. *Scientific Reports*, 5, 16498–19. doi:10.1038/srep16498